Otoacoustic emissions predict cochlear-nerve but not behavioral frequency tuning in an avian vocal-communication specialist

Abbreviated title: Otoacoustic estimation of avian frequency tuning

Diana M. Karosas,[1] Leslie Gonzales,[2] Yingxuan Wang,[1] Christopher Bergevin,[4] Laurel H. Carney,[1,2] and Kenneth S. Henry[1,2,3]

Departments of [1]Biomedical Engineering, [2]Neuroscience, and [3]Otolaryngology, University of Rochester, Rochester, NY 14642

[4]Department of Physics and Astronomy, York University, Toronto, ON, M3J 1P3, Canada

Correspondence should be addressed to Kenneth S. Henry at kenneth_henry@urmc.rochester.edu

The authors declare no competing financial interests.

Acknowledgements

This research was supported by R01-DC017519 and R01-DC001641 from the National Institute on Deafness and Communication Disorders. Discussions with Natasha Mhatre are gratefully acknowledged.

Abstract

Frequency analysis by the cochlea forms a key foundation for all subsequent auditory processing. Stimulus-frequency otoacoustic emissions (SFOAEs) are a potentially powerful alternative to traditional behavioral experiments for estimating cochlear tuning without invasive testing, as is necessary in humans. Which methods accurately predict cochlear tuning remains controversial due to only a single animal study comparing SFOAE-based, behavioral, and cochlear frequency tuning in the same species. The budgerigar is a parakeet species with human-like behavioral sensitivity to many sounds and the capacity to mimic speech. Multiple studies show that budgerigars exhibit a perceptual "auditory fovea" with sharpest behavioral frequency tuning at mid frequencies from 3.5-4 kHz, in contrast to the typical pattern of monotonically increasing tuning sharpness for higher characteristic frequencies. We measured SFOAE-based and cochlear-afferent tuning in budgerigars, for comparison to previously reported behavioral results. SFOAE-based and cochlear-afferent tuning sharpness both increased monotonically for higher frequencies, in contrast to the behavioral pattern. Thus, SFOAE-based tuning in budgerigars accurately predicted cochlear tuning, and both measures aligned with typical patterns of cochlear frequency tuning in other species. Given divergent behavioral tuning in the budgerigars, which could reflect specializations for central processing of masked signals, these results highlight the value of SFOAEs for estimating cochlear tuning and caution against direct inference of cochlear tuning from behavioral results.

Introduction

Cochlear frequency tuning provides the foundation for tonotopic processing by the auditory system (Bourk et al., 1981; Schreiner and Langner 1997; Song et al., 2024). Otoacoustic emissions (Kemp, 1978) and behavioral testing (Moore, 1978) are two methods currently available to evaluate cochlear tuning in humans, for which direct measurement is not possible. Which methods accurately predict cochlear tuning remains controversial due to limited studies comparing otoacoustic, behavioral, and cochlear tuning in the same species.

Stimulus-frequency otoacoustic emissions (SFOAEs) are low-level acoustic signals

recorded in response to tones that depend on active processes within the cochlea (Kemp, 1978; Shera and Guinan, 1999). SFOAE delay is expected to vary with cochlear tuning sharpness based on filter theory, with longer delays implicating sharper tuning. Previous studies found long SFOAE delays in humans, consistent with exceptional tuning sharpness (Shera et al., 2002). However, otoacoustic tuning estimation remains an indirect approach requiring validation. Behavioral experiments infer tuning from masking patterns, typically based on variation in tone thresholds across maskers differing in spectral content (Moore, 1978). However, behavioral tuning estimates depend on central processing of noisy signals in addition to cochlear tuning, and results vary across stimulus paradigms with active debate as to which methods better approximate actual tuning (Oxenham and Shera, 2003; Ruggero and Temchin, 2005; Leschke et al., 2022). Whether otoacoustic or behavioral methods provide closer estimates of actual cochlear frequency tuning remains unknown.

Several reports in nonhuman species have tested the extent to which SFOAE delays predict tuning of auditory-nerve responses at the output of the cochlea (Shera et al., 2010; Joris et al., 2011; Bergevin et al., 2015). These studies found that auditory-nerve tuning quality exceeds N_{SFOAE} (SFOAE delay in stimulus cycles) by a "tuning ratio" that decreases from ~3 to 1 from apex to base across several species (Shera et al., 2010). To our knowledge, only a single study has compared SFOAE and behavioral tuning estimates to auditory-nerve recordings in the same species, ferret (Sumner et al., 2018). SFOAE-based, behavioral, and auditory-nerve tuning quality in ferret all increased monotonically for higher frequencies, in broad accordance with one another (Sumner et al., 2018). A stronger test of SFOAE vs. behavioral tuning estimates could be obtained by studying species with specialized behavioral and/or physiological frequency-resolving abilities.

The budgerigar (*Melopsittacus undulatus*) is a parakeet species with well-known auditory processing abilities from behavioral studies (Dooling et al., 1989, 2000; Ryals et al., 2013; Henry et al., 2016, 2017; Wong et al., 2019; Henry and Abrams, 2024). Intriguingly, many studies show non-monotonic frequency dependence of tuning sharpness in budgerigars, with sharpest tuning at mid frequencies from 3.5-4 (Dooling et al., 2000; Fig. 1). Suggestive of an "auditory fovea" (Köppl et al., 1993), the pattern contrasts with the typical monotonic growth of tuning sharpness frequency in other species. In budgerigars, directly measured critical bands and psychophysical tuning curves based on multiple paradigms (Fig. 1) all indicate peak tuning sharpness from 3-4

kHz near the midpoint of this species' audible frequency range (see also budgerigar critical ratios: Dooling and Saunders, 1975; Okanoya and Dooling, 1987; Farabaugh et al., 1988). Because auditory-nerve tuning has not been measured, it remains unknown whether budgerigars' unusual behavioral tuning reflects specialized cochlear tuning, and if so, whether the pattern is detectable using SFOAEs.

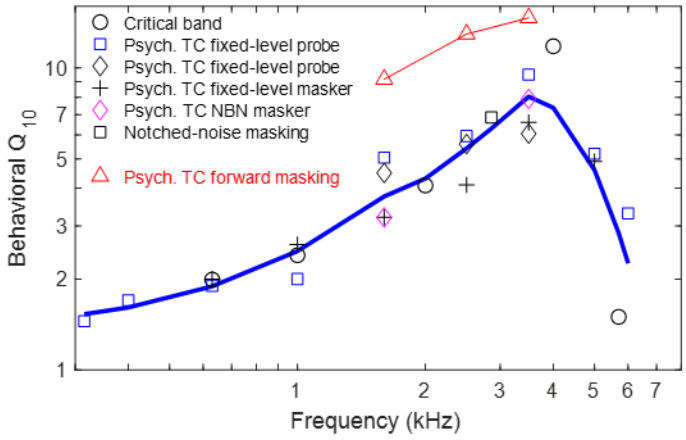

Figure 1. Behavioral frequency tuning in the budgerigar. Published behavioral studies employing multiple stimulus paradigms indicate a peak in behavioral tuning sharpness from 3.5-4 kHz. Red triangles are based on forward masking (Kuhn and Saunders, 1980); all other symbols indicate simultaneous masking results (black circles: Saunders et al., 1978; blue squares: Saunders et al., 1979; black diamonds: Kuhn and Saunders, 1980; black crosses: Saunders and Pallone, 1980; magenta diamonds: Saunders et al., 1979; black square: Dooling et al., 2000). The blue line is a LOESS fit to the simultaneous-masking results with a smoothing parameter of 0.65. TC: tuning curve; NBN: narrowband noise.

The present study compared the extent to which SFOAE and behavioral tuning measures predict actual cochlear tuning in budgerigars, a species that does not show typical monotonic growth of behavioral tuning sharpness with increasing frequency (Fig. 1). SFOAE-based tuning, estimated with low-level swept-tone stimuli, was compared to measures of auditory-nerve tuning and to previously reported behavioral measures of frequency tuning. In budgerigars, SFOAE and auditory-nerve tuning sharpness both increased monotonically with frequency, as in most other species, and in contrast to previously reported behavioral results. Thus, SFOAE delay predicted auditory-nerve tuning sharpness with greater accuracy than behavioral masking approaches.

Materials and Methods

Animals. Budgerigars were sourced from a breeder or our institutional breeding program. SFOAEs were recorded from 22 ears in 14 budgerigars (7 female). Birds were 6 to 32 months old with a median age of 8.5 months at the time of SFOAE experiments. Auditory-nerve responses were recorded from 5 ears in 5 budgerigars (3 female). Birds were 6 to 22 months old at the time of the auditory-nerve recordings (median: 7.5 months). All experiments were approved by the University of Rochester Committee on Animal Resources.

SFOAE recordings. Animals were anesthetized for SFOAE recordings by subcutaneous injection of 0.08–0.12 mg/kg dexmedetomidine and 3–5.8 mg/kg ketamine. Following anesthesia, birds were placed in a stereotaxic apparatus located inside a double-walled acoustic isolation booth (Industrial Acoustics; 2 × 2.1 × 2.2 m). Temperature was maintained at 40°C throughout the experiment using a feedback-controlled heating pad (Harvard Apparatus Model 50-753, Edenbridge, KY, USA). Careful control of temperature was found to be critical for robust emission measurements. Breathing rate was monitored using a thermistor-based sensor.

After birds were placed in the stereotactic apparatus, a probe assembly consisting of a low-noise microphone (Etymotic ER10-B+, Elk Grove Village, IL, USA) and two earphones (Etymotic ER2, Elk Grove Village, IL, USA) was sealed to the ear using ointment. Acoustic stimuli were generated in MATLAB (The MathWorks, Natick, MA, USA; 50-kHz sampling frequency) and processed with a digital pre-emphasis filter (5000-point FIR) that corrected for the frequency response (i.e., magnitude and phase) of the system. The frequency response of the system was measured with the probe microphone at 249 linearly spaced frequencies (1-V peak amplitude) from 0.05-15.1 kHz. Stimuli were converted to analog at maximum scale (10-V peak amplitude; National Instruments PCIe-6251, Austin, TX, USA), attenuated to the required levels (Tucker Davis Technologies PA5, Alachua, FL, USA), and amplified using a headphone buffer (Tucker Davis Technologies HB7).

Stimuli for measuring SFOAEs were swept tones, as in Kalluri and Shera (2013). Two distinct acoustic signals were presented: a probe and a suppressor. The probe consisted of a tone linearly swept at a constant rate from 500 Hz to 8 kHz over 2.05 s, presented at 40 dB SPL. The suppressor consisted of a tone swept at a constant rate from 540 Hz to 8.04 kHz over 2.05 s,

presented at 55 dB SPL. Stimuli were presented in repeating sequences in which the probe was presented first, then the suppressor, and finally the probe and the suppressor simultaneously. All stimuli had 25-ms raised-cosine onset and offset ramps. Each experiment consisted of forty repetitions of the stimulus sequence. There was a half-second silent time gap between presentations of each stimulus sequence. Response waveforms were amplified by 40 dB (Etymotic ER10B+) prior to sampling at 50-kHz and storage on a computer hard drive.

After the completion of the experiments, birds were given a subcutaneous injection of 0.5 mg/kg atipamezole and placed in a heated recovery chamber until fully alert.

Auditory-nerve recordings. The surgical procedures for neurophysiological recordings in budgerigars have been described previously (Wang et al., 2021). Equipment is described above in the section on SFOAE recordings, except where noted. Briefly, animals were anesthetized with a weight-dependent subcutaneous injection of ketamine and dexmedetomidine, as indicated above, and a head-post was mounted to the dorsal surface of the skull with dental cement to facilitate head positioning. Animals were placed in a stereotaxic device inside a sound-attenuating chamber, with the beak projected downward. The right ear was aligned with an earphone/microphone assembly and sealed with silicone grease. Body temperature was maintained at 40°C using a homeothermic control unit, and breathing rate was monitored throughout experiments. Animals were maintained in an areflexic state through continuous subcutaneous infusion of additional ketamine (3-10 mg/kg/h) and dexmedetomidine (0.08-0.2 mg/kg/h), along with physiological saline, using a syringe pump. DPOAEs were recorded periodically throughout experiments to test for possible deterioration of inner-ear function (Wong et al., 2019). Animals were euthanized at the conclusion of recordings, typically after 10-12 hours.

Access to the auditory nerve was accomplished by aspirating the right third of the cerebellum to reveal stereotaxic landmarks associated with the anterior semicircular canal. Recordings were made using pulled glass microelectrodes with 10-80 MΩ impedance. The tip of the electrode was positioned just anterior to a bony spur located on the medial surface of the ampulla of the anterior canal, and advanced into the brainstem using a hydraulic oil-filled remote microdrive (Drum drive; FHC, Bowdoin, ME, USA). Neurophysiological activity was amplified (variable gain; Grass P511 AC amplifier and high-impedance headstage), filtered from 0.03-3

kHz, and broadcast to the experimenters (outside the booth) over a monitor speaker. Action potentials were detected with a custom spike-discriminator circuit consisting of a Schmitt trigger followed by a peak detector and timed with National Instruments hardware. A wideband-noise search stimulus was used to isolate auditory-nerve fibers as the electrode was slowly advanced. Recordings were excluded as likely originating from nucleus angularis based on bipolar action potential morphology, non-primary-like post-stimulus time histograms in response to tones (i.e., onset or chopping responses), or weak phase locking to tones.

Tuning curves were determined through an automated algorithm that tracked the threshold sound level for rate excitation across frequencies. The algorithm estimated thresholds as the minimum tone level that repeatedly produced an increase in driven discharge rate compared to the most recent silent interval (Chintanpalli and Heinz, 2007). Tones were 50 ms in duration with 5-ms raised-cosine onset and offset ramps, presented once every 100 ms. Thresholds were sampled with a resolution of 28 frequencies per octave near characteristic frequency (CF), starting at 6-8 kHz and proceeding downward in frequency (typical range: 6 kHz to 200 Hz).

SFOAE processing. Analyses were performed in MATLAB R2023a and R version 4.3.2. Occasional microphone-signal artifacts were rejected by thresholding. Surrounding each signal transient artifact, 20 ms of signal was removed. Responses to the probe, suppressor, and combined probe and suppressor were isolated by indexing. SFOAEs were calculated by vector subtraction (Shera et al., 2002), as indicated in Eqn. 1, where P is the response waveform in Pa and subscripts denote the stimulus class. Responses were averaged over the 40 repetitions per experiment for P_{SFOAE} calculation.

$$P_{SFOAE} = P_{Probe} - P_{Suppressor} + P_{Probe+Suppressor} \qquad (1)$$

The noise floor was estimated by the spectrum of the difference between odd and even trials of SFOAEs. Magnitude and phase spectra were extracted from the mean data for each component of the signal using the generalized least-squares fit described in Long and Talmadge (1997) and Long et al. (2008). Phase gradients were extracted after phase unwrapping and conversion to cycles.

Two exclusion criteria were implemented prior to phase-gradient extraction, for N_{SFOAE} estimation. Data points less than 10 dB in magnitude above the median of the estimated noise floor (Fig. 2a, gray shaded region) were rejected. Data points at the base of magnitude troughs were also rejected due to noted phase irregularities. Similar algorithms have previously been applied (e.g., Shera and Bergevin, 2012) to emphasize phase-gradient delays near magnitude maxima.

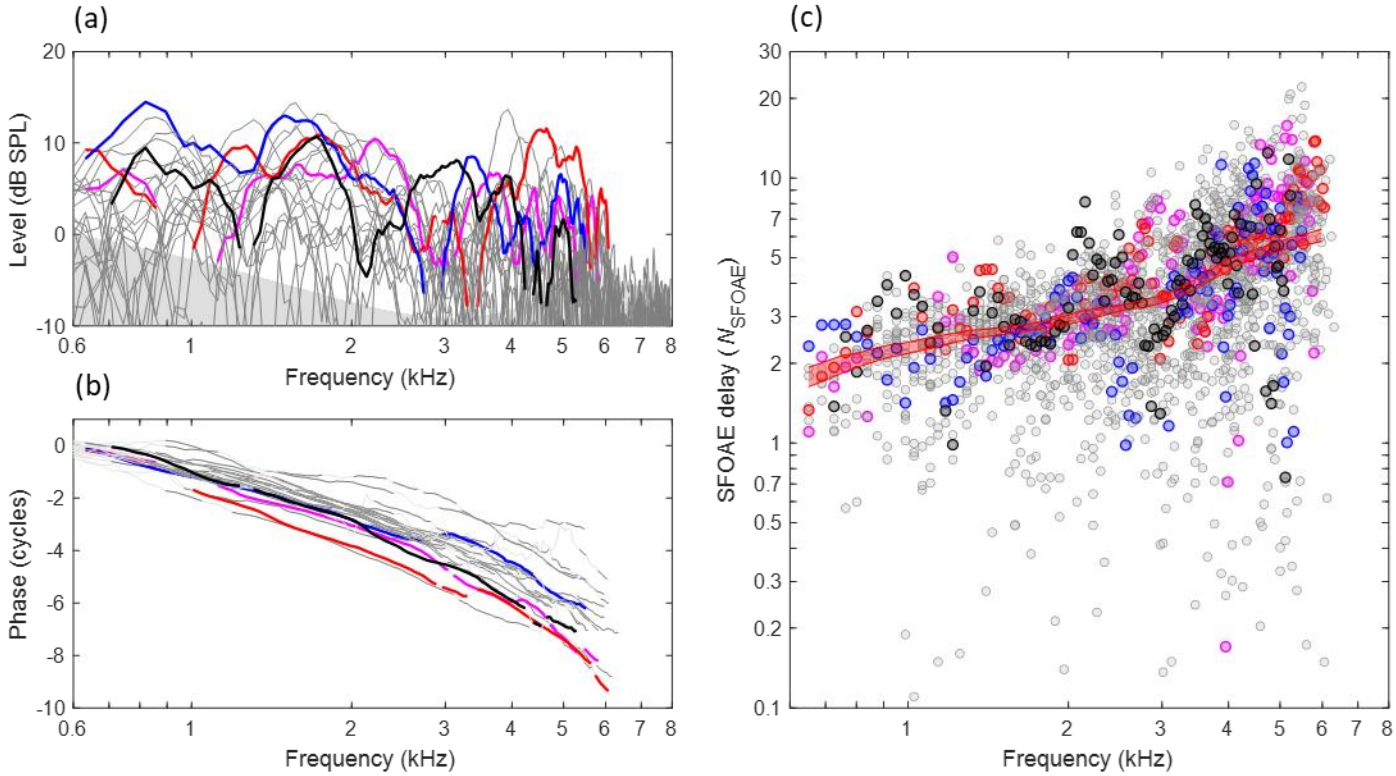

Figure 2. Budgerigar stimulus-frequency otoacoustic emissions (SFOAEs) of 22 ears in 14 animals. (a) SFOAE level ranged from 5-15 dB at stimulus frequencies from 0.6-6 kHz, showing multiple spectral notches within this frequency range, and descended into the noise floor (gray shaded region) at higher frequencies. Thick colored lines highlight SFOAE level in four representative ears. (b) SFOAE phase decreased monotonically for higher stimulus frequencies. (c) SFOAE delay in stimulus cycles, N_{SFOAE}, calculated from individual phase gradients in (b). The shaded region shows the 95% confidence interval of the weighted median (Gaussian weighting function; sigma: 0.25 octaves; 1,000 bootstrap repetitions). Data from the same representative ear are presented in the same color across panels.

Auditory-nerve response processing. Auditory-nerve tuning curves were first smoothed with a 5-point triangular window. CF was calculated as the frequency of the lowest threshold, Q_{10} was calculated as CF divided by the tuning curve bandwidth 10 dB above the lowest threshold, and Q_{ERB} (i.e., the tuning quality of the idealized rectangular filter with equivalent bandwidth to the measured tuning curve) was calculated based on the area under the inverted tuning curve, as in Bergevin et al. (2015).

Statistical analysis. Linear mixed-effects models were implemented to determine the effect of frequency on SFOAE magnitude and phase-gradient responses. Magnitude and N_{SFOAE} values were grouped into five log-spaced frequency bands, with center frequencies ranging from 1 to 5 kHz. For each ear, first-degree robust polynomials were fit to the data in each frequency band. Magnitude and phase-gradient values were defined as the value of the polynomial fit at the center frequency in each band. Frequency was treated as a categorical variable. Ear intercepts were modeled as a random effect. The Satterthwaite approximation was used to calculate degrees of freedom for F tests. Statistical analyses were conducted with a significance level of $\alpha = 0.01$.

Results

Budgerigar SFOAEs

SFOAEs were recorded from 22 ears in 14 animals using swept-frequency tones presented at 40 dB SPL. SFOAE level (Fig. 2a) typically ranged from 5-15 dB at stimulus frequencies below 5-6 kHz and descended into the noise floor at higher frequencies. Within the frequency of measurable emissions, SFOAEs in individual ears (Fig. 2a, colored lines) typically showed three or more deep spectral notches in emission level. Frequency regions near spectral notches, or for which SFOAE level was within 10-dB of the estimated noise floor, were excluded from subsequent analyses as described above (see II. METHODS. D. SFOAE processing). SFOAE phase decreased monotonically with increasing frequency and was relatively consistent across individual ears (Fig. 2b). Finally, SFOAE delay was estimated from the phase gradient of the response and expressed in stimulus cycles, i.e., as N_{SFOAE} (Fig. 2c). So calculated, N_{SFOAE}

increased monotonically with increasing frequency, consistent with gradually increasing tuning quality along the length of the cochlea from apex to base.

Linear mixed-effect modeling revealed a significant effect of frequency on SFOAE level ($F_{4,84} = 18.91$, $p < 0.0001$), associated with slightly lower SFOAE level in the higher frequency bands. Moreover, a linear mixed-model analysis of N_{SFOAE} revealed a significant effect of frequency ($F_{4,84} = 44.05$, $p < 0.0001$) due to greater N_{SFOAE} in higher frequency bands. In summary, SFOAE results pooled across ears were consistent with monotonically increasing tuning sharpness from the cochlear apex to base.

Auditory-nerve tuning curves

Auditory-nerve tuning curves (n=107) in budgerigars had CFs ranging from 0.34-5.65 kHz (median: 3.28 kHz; interquartile range: 2.01-4.00 kHz) and associated thresholds at CF as low as 5 dB SPL (Fig. 3a, crosses). Individual tuning curves (Fig. 3a, colored lines) appeared symmetric around CF on a log-frequency axis, with no clear indication of a secondary tail region of low-frequency sensitivity for stimulus levels up to 80 dB SPL (i.e., the highest level tested). Q_{10}, the measure of tuning-curve sharpness, increased monotonically and significantly for higher CFs (Fig. 3b; $t_{105}=5.351$, $p<0.0001$; t-test of linear regression slope between log-transformed variables) as in other animal species, without an apparent peak at 3.5-4 kHz. Q_{ERB} also increased monotonically for higher CFs (Fig. 4a).

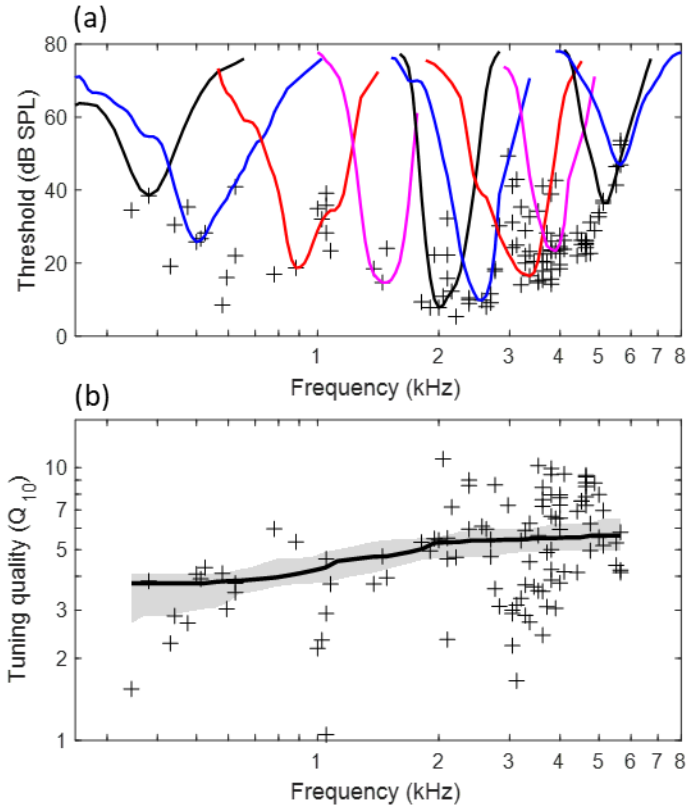

Figure 3. Budgerigar auditory-nerve recordings from 104 fibers in 5 animals. (a) Representative tuning curves (colored lines) show the threshold for excitation of the neural response as a function of tone frequency. Tuning curves are V-shaped and are approximately symmetrical around CF on a log-frequency axis. Black crosses show the threshold at the characteristic frequency (CF) for all recorded fibers. (b) Tuning-curve Q_{10} increases for higher CFs across the neural population. The black trend line and gray shaded region show the weighted median Q_{10} (Gaussian weighting function; sigma: 1 octave) and 95% confidence interval (1,000 bootstrap repetitions), respectively.

Comparison of SFOAE, auditory-nerve, and behavioral measures of frequency selectivity

N_{SFOAE} values expressing SFOAE delay were less than the Q_{ERB} of auditory-nerve tuning curves at the same frequency (Fig. 4a, compare red and black trend lines), by a factor that decreased from ~3.5 for frequencies from 0.7-3 kHz to 1.79 at 5.5 kHz (Fig. 4b, continuous black line). Previous studies (e.g., Shera et al., 2002, 2010) quantified this difference with a scaling factor or "tuning ratio," *r*, assumed to vary slowly with frequency and fit to the empirically derived quotient of auditory-nerve Q_{ERB} and N_{SFOAE}, as indicated in Eqn. 2.

$$r = \frac{Q_{ERB}}{N_{SFOAE}} \quad (2)$$

The tuning ratio in budgerigars was well approximated by log-linear function that decreased from 3.582 at 1000 Hz by 0.6617 per octave increase in frequency (Fig. 4b, dashed line; i.e., $r = -0.6617*\log_2(f/1000) + 3.582$, where f is the SFOAE frequency in Hz). Scaling of N_{SFOAE} by this log-linear function produced SFOAE tuning estimates that closely matched auditory-nerve Q_{ERB} across the full range of SFOAE frequencies investigated (Fig. 4a, magenta line).

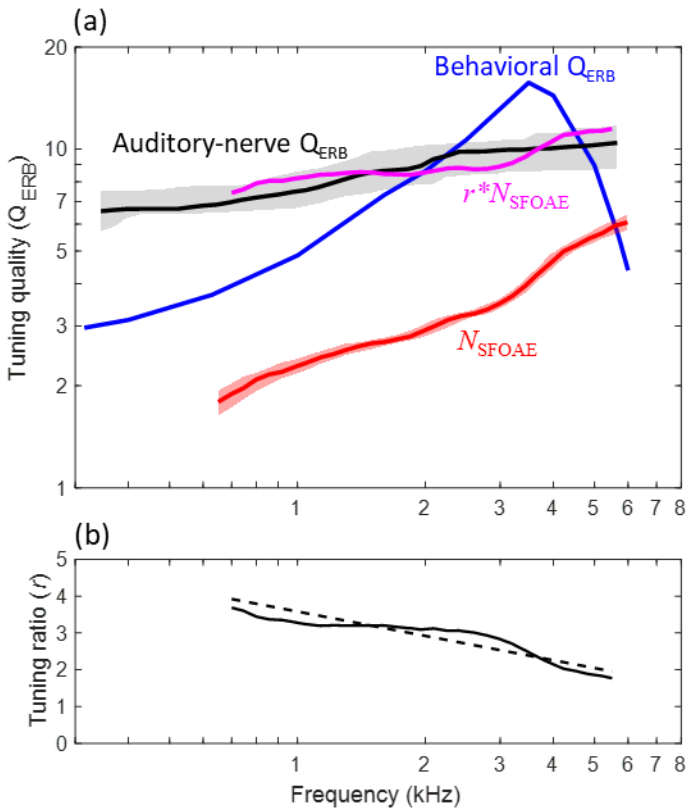

Figure 4. Comparison of SFOAE, auditory-nerve, and behavioral measures of frequency tuning. (a) Budgerigar N_{SFOAE}, auditory-nerve Q_{ERB}, $r*N_{SFOAE}$, and behavioral Q_{ERB} plotted as a function of frequency. Scaling of N_{SFOAE} by r produces a good fit to the observed auditory-nerve Q_{ERB} values (magenta line), whereas behavioral Q_{ERB} shows an entirely different profile. (b) Observed values of the tuning ratio, r, calculated as the quotient of Q_{ERB} and N_{SFOAE} (continuous line), and the fitted parametric expression (dashed line). Shaded regions in (a) indicate 95% confidence intervals of weighted medians estimated with 1,000 bootstrap repetitions.

The otoacoustic and auditory-nerve estimates of peripheral frequency tuning, plotted together with the average behavioral tuning sharpness in this species (Fig. 4a), highlight the similarities and differences across these measures. Behavioral Q_{10} values from the literature (Fig. 1) were scaled by a factor of 1.945 to estimate Q_{ERB}, based on the mathematical expression for the equivalent rectangular filter (Verschooten et al., 2012). Whereas otoacoustic and auditory-nerve measures of tuning quality all increased monotonically with increasing frequency, the behavioral results show a fundamentally different pattern, characterized by a distinct peak from 3.5-4 kHz. Thus, N_{SFOAE} predictions agreed more closely with auditory-nerve tuning quality than with behaviorally estimated frequency tuning in the budgerigar.

Discussion

The present study measured SFOAEs in budgerigars to estimate cochlear frequency tuning. SFOAEs were recorded from 22 budgerigar ears. Tuning curves were also recorded from budgerigar single auditory-nerve fibers for direct comparison. SFOAE level remained above the noise floor for frequencies below 6 kHz and trended downward with increasing frequency. SFOAE delay expressed as N_{SFOAE} increased steadily for higher stimulus frequencies, consistent with increasing tuning quality along the length of the cochlea in the 650 Hz - 6 kHz range. Tuning curves of auditory-nerve fibers concurred with otoacoustic measures of frequency tuning in displaying approximately monotonically increasing Q_{10} and Q_{ERB} with increasing CF across the range of CFs encountered, from 0.34-5.65 kHz. In contrast, previous behavioral studies of budgerigar psychophysical tuning curves, critical bands, and iso-level masking function highlight a prominent peak in tuning sharpness from 3.5-4 kHz suggestive of an auditory fovea (Dooling and Saunders, 1975; Saunders et al., 1978, 1979; Saunders and Pallone, 1980; Kuhn and Saunders, 1980). Overall, the results show that SFOAE delays in budgerigars are more predictive of auditory-nerve tuning sharpness than previously reported behavioral frequency tuning estimates based on masking.

Auditory-nerve tuning and N_{SFOAE} have been shown to covary with frequency in monkeys (Joris et al., 2011), chinchillas (Shera et al., 2010), geckos (Bergevin and Shera, 2010), cats and guinea pigs (Shera et al., 2002), ferrets (Sumner et al., 2018), and barn owls (Bergevin et al.,

2015). The present study concurs with these findings across species, showing agreement between auditory-nerve and otoacoustic measures of frequency tuning. N_{SFOAE} and auditory-nerve Q_{10} or Q_{ERB} values both indicated approximately monotonically increasing tuning sharpness along the budgerigar cochlea from apex to base. That the N_{SFOAE} trendline was below the Q_{ERB} values has been observed in previous studies (mammals: Shera et al., 2010; Sumner et al., 2018; birds: Bergevin et al., 2015), and may partly reflect the level-dependence of SFOAEs. Although the present study did not explore the level-dependence of SFOAEs in the budgerigar, lower probe sound levels have been shown to yield larger N_{SFOAE} values in other species (e.g. barn owl; Bergevin et al., 2015). Reducing the probe sound level may raise the N_{SFOAE} trendline closer to the Q_{ERB} trendline but would also decrease SFOAE level.

Previous studies (e.g., Shera et al., 2010) established the concept of a tuning ratio, defined as the quotient Q_{ERB}/N_{SFOAE}, that can be applied as a scalar to N_{SFOAE} to predict cochlear tuning sharpness. The tuning ratio in budgerigars decreased from ~3.5 for frequencies from 0.7-3 kHz to 1.79 at 5.5 kHz. These values are similar to, but near the high end of, previously reported tuning ratios in mammalian species, which decrease from approximately 3 to 1 from apex to base in cat, guinea pig, and chinchilla (Shera et al., 2010). In birds, tuning ratios of the barn owl show an intriguing minimum at 6 kHz, approaching 1 from values near 2 at higher and lower frequencies (Bergevin et al., 2015), and unpublished SFOAE data from chickens suggest fairly high tuning ratios, decreasing from perhaps 8 to 2 from apex to base (but note that precise estimation is hampered by variability of auditory-nerve tuning measurements across studies; Manley et al., 1991; Salvi et al., 1992; Saunders et al., 1996). Because the tuning ratio is such a key parameter in otoacoustic estimation of cochlear frequency tuning, further studies of taxonomic variation in tuning ratios and its physiological basis is highly warranted (Bergevin et al., 2008; Manley 2022).

The estimates of behavioral frequency selectivity referenced in the present study were originally obtained using three simultaneous masking paradigms: psychophysical tuning curves for probe-tone detection in tonal or narrowband maskers, critical bands for tone detection in bandlimited noise, and critical ratios for tone detection in wideband noise (Dooling and Saunders, 1975; Saunders et al., 1978, 1979; Saunders and Pallone, 1980; Kuhn and Saunders, 1980; Dooling et al., 2000). All three behavioral measures show that perceptual frequency selectivity in budgerigars is greatest from 3.5-4 kHz and declines markedly at higher and lower

frequencies. Suggestive of a perceptual auditory fovea, this pattern differs substantially from behavioral findings in humans and other model species, which show monotonically increasing behavioral frequency selectivity for higher frequencies. Critically, the behavioral findings contrast with physiological tuning estimates of the current study, which show monotonically increasing SFOAE phase gradients with increasing frequency as well as monotonically increasing auditory-nerve Q_{10}/Q_{ERB} values for high CFs. Thus, neither SFOAEs nor auditory-nerve recordings suggest the existence of a peripheral auditory fovea that could explain prior behavioral findings in this species.

While the reason for disparate behavioral and SFOAE/auditory-nerve findings in budgerigars is unknown, the mismatch highlights the need for caution in inferring cochlear frequency selectivity using behavioral measures. Indeed, previous work in humans has shown that simultaneous masking paradigms can result in behavioral tuning functions that are qualitatively and quantitatively distinct from otoacoustic measures (Shera et al., 2002). Shera et al. (2002) and Sumner et al. (2018) demonstrated in humans and ferrets, respectively, that revised psychophysical paradigms designed to reduce the effects of nonlinear suppression and compression can yield behavioral results that more closely resemble otoacoustic measures. On the other hand, Ruggero and Temchin (2005) argued that forward-masking behavioral paradigms can substantially overestimate cochlear frequency selectivity. Moreover, psychophysical tuning curves obtained with forward masking in budgerigars (Kuhn and Saunders, 1980) have Q_{10} values that are greater than twice simultaneous-masking values at the same frequencies (Fig. 1; red triangles), while also far exceeding the maximum auditory-nerve Q_{10} values reported in Fig. 3. In summary, at least in budgerigars, it appears unlikely that any of the previously employed forward or simultaneous masking paradigms reasonably estimate cochlear frequency selectivity in this species.

A potential explanation for the disparity between behavioral and the other measures of frequency tuning lies in the nature of the measurements. Otoacoustic and auditory-nerve responses both reflect peripheral physiological processes originating in the cochlea. However, behavioral measures of frequency selectivity necessarily involve the entire auditory pathway and central nervous system, including neural mechanisms for processing masked signals, and are best explained by models that include both peripheral and central auditory system processes (Maxwell et al., 2020; Brennan et al., 2023). The unique pattern observed in the budgerigar's

behavioral Q_{10} trendline may then reflect specializations for masked processing in the central auditory pathway of this highly vocal and gregarious species. While a previous study investigated neural tone-in-noise processing in the budgerigar's inferior colliculus, the study did not explore the impact of noise bandwidth on neural detection thresholds (Wang et al., 2021; which would be needed to estimate neural critical bands). Note that the frequency selectivity of inferior colliculus response maps obtained with single tones of varying frequency and level showed no obvious peak in tuning quality for neural CFs from 3.5-4 kHz (Henry et al., 2016, 2017), similar to the present auditory-nerve results. Finally, several histological studies of budgerigar cochlear morphology also revealed no obvious specializations consistent with a peripheral auditory fovea (Manley et al., 1993; Wang et al., 2023)

In conclusion, SFOAE-based and auditory-nerve measures of tuning sharpness increased for higher frequencies in the budgerigars. The pattern is similar to findings in other avian and mammalian species, and contrasts with the unusual pattern of behavioral frequency tuning in budgerigars, which has maximum tuning quality from 3.5-4 kHz consistent with an auditory fovea. These results highlight the need for caution in interpreting behavioral measures of frequency tuning, which can show substantial deviation from cochlear tuning curves due to central processing mechanisms and other factors that necessarily influence behavioral detection of masked signals.

References

Bergevin C, Freeman DM, Saunders JC, Shera CA (2008) Otoacoustic emissions in humans, birds, lizards, and frogs: evidence for multiple generation mechanisms. J Comp Physiol A 194: 665–683.

Bergevin C, Manley GA, Köppl C (2015) Salient features of otoacoustic emissions are common across tetrapod groups and suggest shared properties of generation mechanisms. Proc Natl Acad Sci USA 112: 3362–3367.

Bergevin C, Shera CA (2010) Coherent reflection without traveling waves: On the origin of long-latency otoacoustic emissions in lizards. J Acoust Soc Am 127: 2398–2409.

Bourk TR, Mielcarz JP, Norris BE (1981) Tonotopic organization of the anteroventral cochlear

nucleus of the cat. Hear Res 4: 215–241.

Brennan MA, Svec A, Farhadi A, Maxwell BN, Carney LH (2023) Inherent envelope fluctuations in forward masking: Effects of age and hearing loss. J Acoust Soc Am 153: 1994–1994.

Chintanpalli A, Heinz MG (2007) Effect of auditory-nerve response variability on estimates of tuning curves. J Acoust Soc Am 122: 203–209.

Dooling RJ, Lohr B, Dent ML (2000) Hearing in Birds and Reptiles. In: Comparative Hearing: Birds and Reptiles (Dooling R.J, Fay RR, Popper AN. eds), pp308-359. New York: Springer.

Dooling RJ, Okanoya K, Brown SD (1989) Speech perception by budgerigars (*Melopsittacus undulatus*): The voiced-voiceless distinction. Percept Psycho 46: 65–71.

Dooling RJ, Saunders JC (1975). Hearing in the parakeet (*Melopsittacus undulatus*): Absolute thresholds, critical ratios, frequency difference limens, and vocalizations. J Comp Physiol Psychol 88: 1–20.

Farabaugh SM, Dent ML, Dooling RJ (1988) Hearing and vocalizations of wild-caught Australian budgerigars (*Melopsittacus undulatus*). J Comp Psychol 112: 74-81.

Henry KS, Abrams KS, Forst J, Mender MJ, Neilans EG, Idrobo F, Carney LH (2017) Midbrain synchrony to envelope structure supports behavioral sensitivity to single-formant vowel-like sounds in noise. J Assoc Res Otolaryngol 18: 165–181.

Henry KS, Guo AA, Abrams KS (2024) Normal behavioral discrimination of envelope statistics in budgerigars with kainate-induced cochlear synaptopathy. Hear Res 441: 108927.

Henry KS, Neilans EG, Abrams KS, Idrobo F, Carney LH (2016) Neural correlates of behavioral amplitude modulation sensitivity in the budgerigar midbrain. J Neurophysiol 115: 1905–1916.

Joris PX, Bergevin C, Kalluri R, Mc Laughlin M, Michelet P, van der Heijden M, Shera CA (2011) Frequency selectivity in Old-World monkeys corroborates sharp cochlear tuning in humans. Proc Natl Acad Sci USA 108: 17516–17520.

Kalluri R, Shera CA (2013) Measuring stimulus-frequency otoacoustic emissions using swept tones. J Acoust Soc Am 134: 356–368.

Kemp DT (1978) Stimulated acoustic emissions from within the human auditory system. J Acoust Soc Am 64: 1386–1391.

Köppl C, Gleich O, Manley GA (1993) An auditory fovea in the barn owl cochlea. J Comp Physiol A 171: 695-704.

Kuhn A, Saunders JC (1980) Psychophysical tuning curves in the parakeet: A comparison between simultaneous and forward masking procedures. J Acoust Soc Am 68: 1892–1894.

Leschke J, Rodriguez Orellana G, Shera CA, Oxenham AJ (2022) Auditory filter shapes derived from forward and simultaneous masking at low frequencies: Implications for human cochlear tuning. Hear Res 420: 108500.

Long GR, Talmadge CL, Lee J (2008) Measuring distortion product otoacoustic emissions using continuously sweeping primaries. J Acoust Soc Am 124: 1613–1626.

Manley GA (2022) Otoacoustic Emissions in Non-Mammals. Audiology Research 12, 260–272.

Manley GA, Kaiser A, Brix J, Gleich O (1991) Activity patterns of primary auditory-nerve fibres in chickens: Development of fundamental properties. Hear Res 57: 1–15.

Manley GA, Schwabedissen G, Gleich O (1993) Morphology of the basilar papilla of the budgerigar, *Melopsittacus undulatus*. J Morphol 218: 153-165.

Maxwell BN, Richards VM, Carney LH (2020) Neural fluctuation cues for simultaneous notched-noise masking and profile-analysis tasks: Insights from model midbrain responses. J Acoust Soc Am 147: 3523–3537.

Moore BCJ (1978) Psychophysical tuning curves measured in simultaneous and forward masking. J Acoust Soc Am 63: 524–532.

Okanoya K, Dooling RJ (1987) Hearing in passerine and psittacine birds: A comparative study of absolute and masked auditory thresholds. J Comp Psychol 101: 7–15.

Oxenham AJ, Shera CA (2003) Estimates of human cochlear tuning at low levels using forward and simultaneous masking. J Assoc Res Otolaryngol 4: 541–554.

Ruggero MA, Temchin AN (2005) Unexceptional sharpness of frequency tuning in the human cochlea. Proc Natl Acad Sci USA 102: 18614–18619.

Ryals BM, Dent ML, Dooling RJ (2013) Return of function after hair cell regeneration. Hear Res 297: 113-20.

Salvi RJ, Saunders SS, Powers NL, Boettcher FA (1992) Discharge patterns of cochlear ganglion neurons in the chicken. J Comp Physiol A 170: 227–241.

Saunders JC, Denny RM, Bock GR (1978) Critical bands in the parakeet (*Melopsittacus undulatus*). J Comp Physiol A 125: 359-365.

Saunders JC, Doan DE, Poje CP, Fisher KA (1996) Cochlear nerve activity after intense sound exposure in neonatal chicks. J Neurophysiol 76: 770–787.

Saunders JC, Pallone RL (1980) Frequency selectivity in the parakeet studied by isointensity masking contours. J Exp Biol 87: 331-342.

Saunders JC, Rintelmann WF, Bock GR (1979) Frequency selectivity in bird and man: A comparison among critical ratios, critical bands and psychophysical tuning curves. Hear Res 1: 303–323.

Schreiner CE, Langner G (1997) Laminar fine structure of frequency organization in auditory midbrain. Nature 388: 383–386.

Shera CA, Guinan JJ (1999) Evoked otoacoustic emissions arise by two fundamentally different mechanisms: A taxonomy for mammalian OAEs. J Acoust Soc Am 105: 782–798.

Shera CA, Guinan JJ, Oxenham AJ (2002) Revised estimates of human cochlear tuning from otoacoustic and behavioral measurements. Proc Natl Acad Sci USA 99: 3318–3323.

Shera CA, Guinan JJ, Oxenham AJ (2010) Otoacoustic estimation of cochlear tuning: validation in the chinchilla. J Assoc Res Otolaryngol 11: 343–365.

Song X, Guo Y, Chen C, Lee JH, Wang X (2024) Tonotopic organization of auditory cortex in awake marmosets revealed by multi-modal wide-field optical imaging. Curr Res Neurobiol 6: 100132.

Sumner CJ, Wells TT, Bergevin C, Sollini J, Kreft HA, Palmer AR, Oxenham AJ, Shera CA (2018) Mammalian behavior and physiology converge to confirm sharper cochlear tuning in humans. Proc Natl Acad Sci USA 115: 11322–11326.

Verschooten E, Robles L, Kovacic D, Joris PX (2012) Auditory nerve frequency tuning measured with forward-masked compound action potentials J Assoc Res Otolaryngol 13: 799–817.

Wang Y, Abrams KS, Carney LH, Henry KS (2021) Midbrain-level neural correlates of behavioral tone-in-noise detection: dependence on energy and envelope cues. J Neurosci 41: 7206.

Wang Y, Abrams KS, Youngman M, Henry KS (2023) Histological correlates of auditory nerve injury from kainic acid in the budgerigar (*Melopsittacus undulatus*). J Assoc Res Otolaryngol 24: 473-485.

Wong SJ, Abrams KS, Amburgey KN, Wang Y, Henry KS (2019) Effects of selective auditory-

nerve damage on the behavioral audiogram and temporal integration in the budgerigar. Hear Res 374: 24–34.